

A bi-layered tubular scaffold for effective anti-coagulant in vascular tissue engineering

Wangchao Yao^{a,1}, Hongbing Gu^{b,1}, Tao Hong^{a,1}, Yao Wang^a, Sihao Chen^d, Xiumei Mo^e, Wenyao Li^f, Chunsheng Wang^a, Tonghe Zhu^{c,*}, Shuyang Lu^{a,*}

^a Department of Cardiovascular Surgery, Zhongshan Hospital, Fudan University, The Shanghai Institute of Cardiovascular Diseases, Shanghai 200032, PR China

^b Department of Cardiovascular Surgery, Shanghai General Hospital, Shanghai Jiao Tong University School of Medicine, Shanghai 200080, PR China

^c Department of Sports Medicine, Department of Orthopedics, Shanghai Jiao Tong University Affiliated Sixth People's Hospital, Shanghai 200233, PR China

^d Multidisciplinary Center for Advanced Materials of Shanghai University of Engineering Science, Shanghai University of Engineering Science, Shanghai 201620, PR China

^e State Key Laboratory for Modification of Chemical Fibers and Polymer Materials, College of Chemistry, Chemical Engineering and Biotechnology, Donghua University, Shanghai 201620, PR China

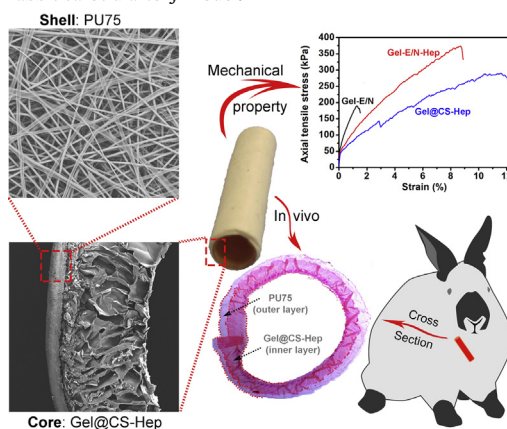
^f Materials Chemistry Centre, Department of Chemistry, University College London, 20 Gordon Street, London WC1H 0AJ, UK

HIGHLIGHTS

- A hybrid bi-layered tubular scaffold were fabricated via a facile freeze-drying combined with amidation.
- The mechanically matched scaffold showed no unfavorable effects on vascular cells and effective anti-acute coagulation properties.
- A novel designed bi-layered vessel prevents acute thrombosis effectively and maintains excellent patency in a rabbit model.

GRAPHICAL ABSTRACT

A hybrid bi-layered vascular scaffold from heparin-grafted gelatin (Gel) and chitosan (CS) composite sponge with porous fluffy inter structure exhibited higher hydrophilicity, stable mechanical properties, especially they demonstrate excellent rapid endothelialization performance and effective anti-acute coagulation properties in rabbit carotid artery model.



ARTICLE INFO

Article history:

Received 10 March 2020

Received in revised form 1 July 2020

Accepted 2 July 2020

Available online 13 July 2020

ABSTRACT

Acute coagulation is one of the vexed problems in transplantation of small-diameter artificial blood vessel. Three-dimensional porous heparin-modified gelatin (Gel)@chitosan (CS) tubular scaffold were successfully acquired by using the method of freeze-drying combined with amidation for application in tissue regeneration of blood vessels. Initially, homogeneous gelatin solution was initially poured into a tubular mold and underwent a procedure of vacuum freeze-drying to form a three-dimensional porous tubular skeleton. Chitosan was used to loading heparin (Hep) which is a kind of efficient anticoagulant. The Hep-loaded CS composite solution were poured into Gel

* Corresponding authors at: No. 1609 Xietu Road, Xuhui District, Shanghai 200032, China.

E-mail addresses: zhutonghe@sjtu.edu.cn (T. Zhu), lu.shuyang@zs-hospital.sh.cn (S. Lu).

¹Wangchao Yao, Hongbing Gu and Tao Hong: These authors contributed equally to this work.

Keywords:

Three-dimensional scaffold
Freeze-drying
Amidation
Anti-acute coagulation
Vascular tissue engineering

tubular skeleton, following freeze-drying matched EDC-NHS crosslinking to form Gel@CS-Hep tubular scaffold exhibited a three-dimensional structure and porous morphology. Then, poly(ester-urethane)urea/gelatin (PU75) micro-nano fibers were electrospinning outside the Gel@CS-Hep tube as mechanical reinforcement layer. The Gel@CS-Hep/PU75 tube showed higher hydrophilicity, stable mechanical properties as well as no cytotoxicity on human umbilical vein endothelial cells. Importantly, the three-dimensional functional Gel@CS-Hep/PU75 tubular scaffold shows a good rapid endothelialization performance and effective anti-acute coagulation properties. Therefore, the developed Gel@CS-Hep/PU75 tube was proposed to be a potential scaffold for remodeling vascular tissue.

© 2020 The Author(s). Published by Elsevier Ltd. This is an open access article under the CC BY license (<http://creativecommons.org/licenses/by/4.0/>).

1. Introduction

Small-diameter artificial blood vessels (inner diameter < 6 mm) are increasingly needed in the clinic for coronary artery bypass grafting, arterial colostomy and repairing of arterial injuries in limbs [1]. Usually, surgical or interventional transplants are often used to treat thrombus, however, acute coagulation will take place after transplantation within a week, especially for small-diameter blood vessel [2]. Anti-acute coagulation and rapid endothelialization are the two huge challenges in small-diameter vascular tissue engineering [3,4]. Therefore, how to make small-diameter artificial blood vessels possess effective and controllable anti-acute coagulation properties also is a major difficulty in vascular tissue engineering. Low molecular weight heparin (LMWH, molecular weight below 6000 D), which often used in clinical for anticoagulant therapy, is a shorter polysaccharide compound isolated from standard heparin, which can inhibit platelet adhesion and aggregation, increases the permeability of blood vessel walls, and regulates angiogenesis [5]. However, the disadvantage of LMWH is that it is not effective in oral administration and has a short duration after administration [6,7]. Therefore, how to design a small-diameter artificial blood vessel with suitable heparin loading and stable sustained-release properties in one week are research bottlenecks that need to be overcome.

To solve the above problems, some researchers have designed a variety of heparin-functional vascular scaffolds based on the three-layer structure of natural blood vessels and the idea of bionics [8–11]. Although some studies in vitro have shown that the prepared vascular scaffolds show good performance, but very few vascular scaffolds can maintain the controllable anticoagulant effect. The key to the reconstruction of vascular tissue successfully is not only to have effective anti-acute coagulation that can get enough time for endothelialization but also to have a three-dimensional structure that can withstand external pressure as well as provide a hotbed for quickly rebuild the functions of blood vessel [12,13].

The natural extracellular matrix of blood vessels included three substances which all were secreted by adjacent cells: protein fiber, proteoglycan, and collagen [14]. These three components are combined by chemical crosslinking or physical crosslinking, where collagen and elastin provide mechanical support for the growth of host cells. Proteins provide sites for each other to bind to other cells and promote cell growth. Gelatin is a various functional group degradation product of collagen (the main component of extracellular matrix) with good biocompatibility, low toxicity, low immune response, which can provide an appropriate physiological environment for cell adhesion, proliferation, migration or differentiation [15–17]. Wang et al. have fabricated vascular grafts that were consisted of a polyurethane fibrous outside-layer and a gelatin-heparin fibrous inner-layer by bilayering electrospinning technology [18]. Although the results shown that PU/gelatin-heparin vascular grafts were less likely to cause thrombosis when used as a substitute for the small-caliber artificial blood vessels, the tiny pore size brought by nanofibers is not suitable for the rapid growth of host cells. Notably, a summary of previous studies of tissue engineering vascular scaffolds, tissue remodeling in scaffolds after implantation can improve the expression of elastin and collagen. This inspired us to remodel

cell-free scaffold with an interconnected porous structure that will accelerate cell migration, infiltration and remodeling [19,20].

In brief, an ideal vascular scaffold for surgical or interventional treatment of cardiovascular diseases should have ideal mechanical properties, compliance matching of autogenous vessels, effective and controllable anti-coagulation properties, and excellent tissue compatibility. In the present research, we will focus on developing a Gel@CS-Hep/PU75 three-dimensional tubular scaffold via facile freeze-drying combined to amidation and electrospinning. The whole preparation strategy is described in Fig. 1. The tubular scaffolds composed of elastic hydrophilic PU75 nanofibers as the outside-layer and hemocompatible three-dimensional porous Gel@CS-Hep as the inner-layer. The release of heparin will show a highly effective anticoagulant effect, which makes the tubular scaffold a potential candidate as a scaffold for artificial blood vessels.

2. Materials and methods

2.1. Materials

Poly(ester-urethane)urea (PEUU) with a weight average molecular weight of 1.5×10^5 was synthesized as shown in previous research [21]. Gelatin (Gel, type B from porcine skin) was purchased from Sigma-Aldrich Chemical Reagent Co., Ltd. (Saint Louis, USA). Chitosan (CS, medical grade, with a degree of deacetylation of $\geq 95\%$ and viscosity of 100–200 mpa-s). Heparin sodium (Hep) with 99.8% purity was obtained from Runcheng Biological Inc. (Shanghai, China). Other related materials and solvents as shown in the attachment in support information.

2.2. Preparation of gel@CS-Hep/PU75 tubular scaffold

2.5 g Gel was dissolved in 50 mL double distilled water with an optimized concentration of 5% (w/v). The prepared sticky Gel solution was poured into the PTFE mold before a simple deaeration using ultrasonic. Then, the obtained assembly was freeze-drying under -80°C for 48 h. Finally, the prepared Gel tubes were soaked in 1-(3-Dimethylaminopropyl)-3-ethylcarbodiimide hydro (EDC)/N-Hydroxy succinimide (NHS) solution or EDC/NHS/Hep activated solution for crosslinking or grafting, respectively, harvested Gel-E/N tube and Gel-E/N-Hep tube.

CS mixed with Hep (4 wt% Hep relative to CS) was dissolved in 100 mL acetic acid solution (1 wt%) with an optimized concentration of 3% (w/v). After that, the crosslinked Gel tubes (Gel-E/N tube) were soaked in the sticky CS/Hep mixture solution following with inflating processing and freeze-drying dispose of as above obtained the Gel@CS-Hep tube.

Finally, blends of PEUU/gelatin with weight ratios of 75/25 were dissolved in HFIP form 5% w/v solutions. The prepared mixture solution was electrospinning on the surfaces of the Gel-E/N, Gel-E/N-Hep, and Gel@CS-Hep tube to harvest the hybrid tubular scaffolds, respectively. During the electrospinning process, a suitable steel rod was inserted into the prepared vascular lumen and fixed in the collector. The outer

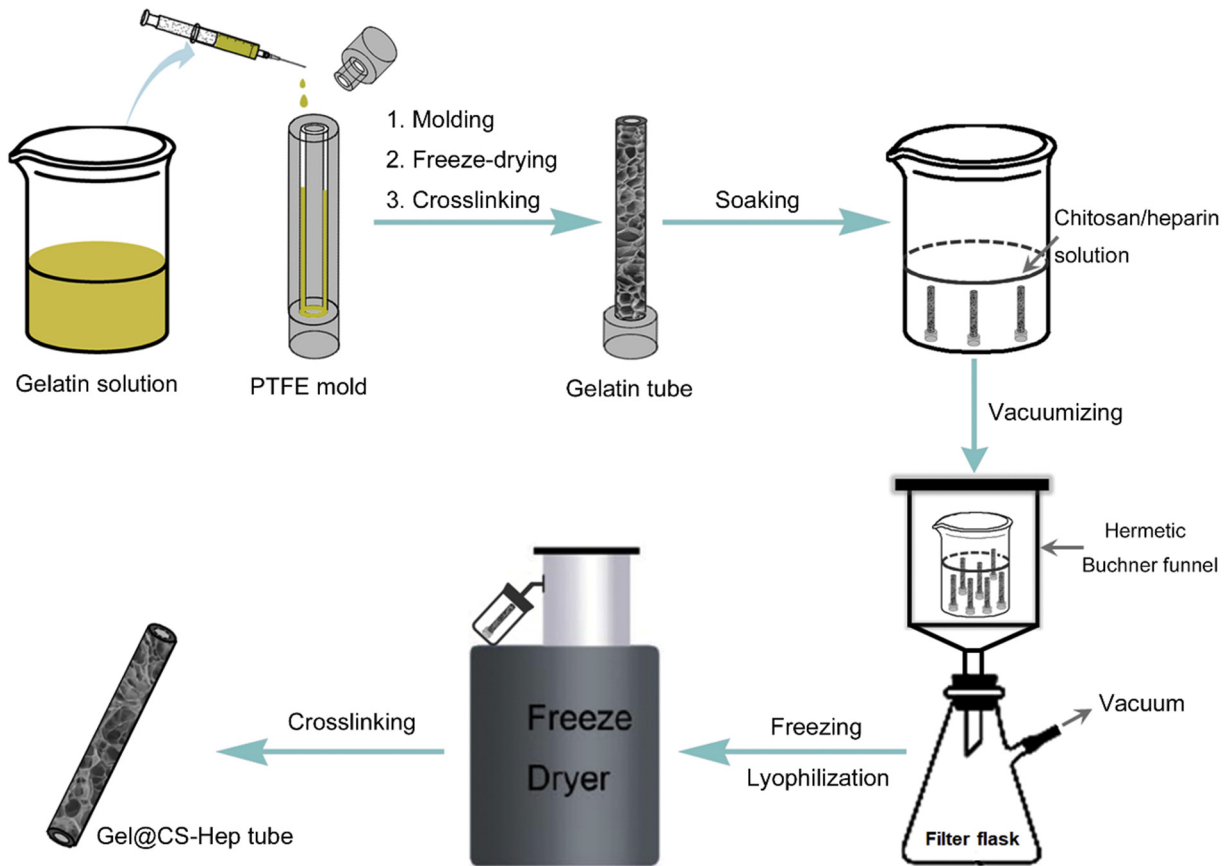


Fig. 1. Schematic of preparation of Gel@CS-Hep tubular scaffold.

layer of the vascular scaffold was prepared with a collection distance of 15 cm at 12 kV and a forward velocity of 1.0 mL/h. The prepared bilayer tubular scaffolds were dried under vacuum for at least 2 days to remove residual solvent.

2.3. The degradation and heparin release of the prepared tubular scaffolds

The density of heparin of prepared tubular scaffolds was measured using the colorimetric method according to the previous report [22,23]. According to the report, toluidine blue stain was utilized in this research. The bilayer tubular scaffolds with heparin-loading (Gel-E/N-Hep tube and Gel@CS-Hep tube) were immersed in the toluidine blue solution at 37 °C for 12 h, then, the tubular scaffolds were washed with distill water. The degree to which the scaffold turns blue represents the density of the scaffold grafted with heparin.

Also, the *in vitro* degradation of the prepared tubular scaffolds was measured during 28 days. Briefly, the initial mass of the scaffold was weighed before soaked in PBS. After that, the scaffold was dried and weighed after taking out at the setting time point to analyze the degradation degree.

Additionally, the heparin sodium standard curve is drawn according to spectrophotometry, and then the heparin-loading tubular scaffold was soaked in 50 mL PBS for at least 7 days releases. Finally, the content of heparin in the sustained release solution was calculated according to the previously determined standard curve.

2.4. Testing of mechanical properties

Basic mechanical performance tests were conducted at room temperature with a fixed stretching speed of 0.02 mm/min [24,25]. In

order to perform the ultimate radial tensile test, tubular specimens were fixed at their cut ends. Five specimens per test were conducted. The stress-strain curves would be recorded while the specimens were extended to rupture.

2.5. Cell experiments and protein absorption evaluation

Human umbilical vein endothelial cells (HUVECs) were applied to evaluate the cytocompatibility of tubular scaffolds [26]. For cell proliferation test, the tubular scaffolds were divided into small discs with a 14 mm diameter and HUVECs were seeded with a density of 1.0×10^4 cells/well. The viability and morphology of the proliferated cells were assessed by Cell counting kit (CCK-8) assay and DAPI (blue)/rhodamine-conjugated phalloidin (red) staining following the manufacturer's protocol, respectively [27].

The sterilized Gel-E/N, Gel-E/N-Hep, and Gel@CS-Hep tube were co-cultured with HUVECs for 12 h, 48 h and 144 h, respectively. At the set time, the incubated tubular scaffolds were taken out from cell culture medium, following with washed three times used PBS. Then, the three types of scaffolds were incubated with 1 mL FBS at 37 °C for 24 h, and the concentrations of FBS before and after adsorption were measured at 280 nm by a protein detection system (GloMax Multi+ *in vitro* protein expression system).

2.6. Implantation in rabbits' carotid artery

Twelve male rabbits, weighing approximately 2.5 kg, were purchased from Shanghai Slaccas Experimental Animal Co., Ltd., Shanghai, China, and two rabbits were in reserve. The unilateral common carotid artery replacement models on rabbits were established for the research. 14 days after the tubular scaffolds were implanted, the Doppler

ultrasonography (VisualSonics, Canada) was taken to evaluate the function of the implants, and then the transplants were harvested and used for hematoxylin and eosin (H&E) staining and immunofluorescent staining analysis.

2.7. Ethics statement

The present study has been approved by the Institutional Animal Care and Use Committee (IACUC). The animal experimental protocols comply with the policy of IACUC of Zhongshan Hospital, Fudan University. The ethical principles were followed throughout all experimental procedures. All animal experiments were performed according to the Animal Management Regulations of China (1988 and revised in 2001, Ministry of Science and Technology).

2.8. Statistical analysis

In all the experiments, at least three samples were performed. Categorical variables are presented as frequencies and percentages, and continuous variables are expressed as mean \pm standard deviation (SD). One-way ANOVA statistical method was used to evaluate the significance of the experimental data. Data were analyzed with SPSS statistical package version 17.0 (SPSS Inc., Chicago, IL, USA), and a value of 0.05 was selected as the significance level, and the data were indicated with (*) for $p < .05$, (**) for $p < .01$, and (***) for $p < .001$, respectively.

3. Results and discussion

As previous research reported, the smaller pore size of the wall of the tubular scaffold may limit the infiltration of host cells as well as limit the regeneration and remodeling of the blood vessel wall [28,29]. Also, the degradation rate of the tubular scaffold is the main factor, which could dominate the effect of vascular reconstruction [30]. Moreover, the long-term sustained host response would cause fibrosis, calcification and intimal hyperplasia of the vascular scaffold [31–33]. We also believe that rapid degradation could provide more space for the penetration, expansion, and formation of the extracellular matrix of the body cells. Therefore, the vascular scaffold with a property of rapid degradation will provide a larger three-dimensional space for cell infiltration, proliferation, and extracellular matrix secretion.

Considering the above, we have designed a bilayer small-diameter tubular scaffold with a connected microporous inner layer and dense fibrous outer layer: The intimal layer of vascular scaffold could be roughly described as 5% gelatin homogeneous solution which was poured into the PTFE molds and followed with freeze-drying and crosslinking-grafting (as depicted in Fig. 1).

3.1. Morphology and surface wettability of scaffolds

It is necessary to characterize the microstructure of the tubular scaffold due to the three-dimensional structure of prepared tubular

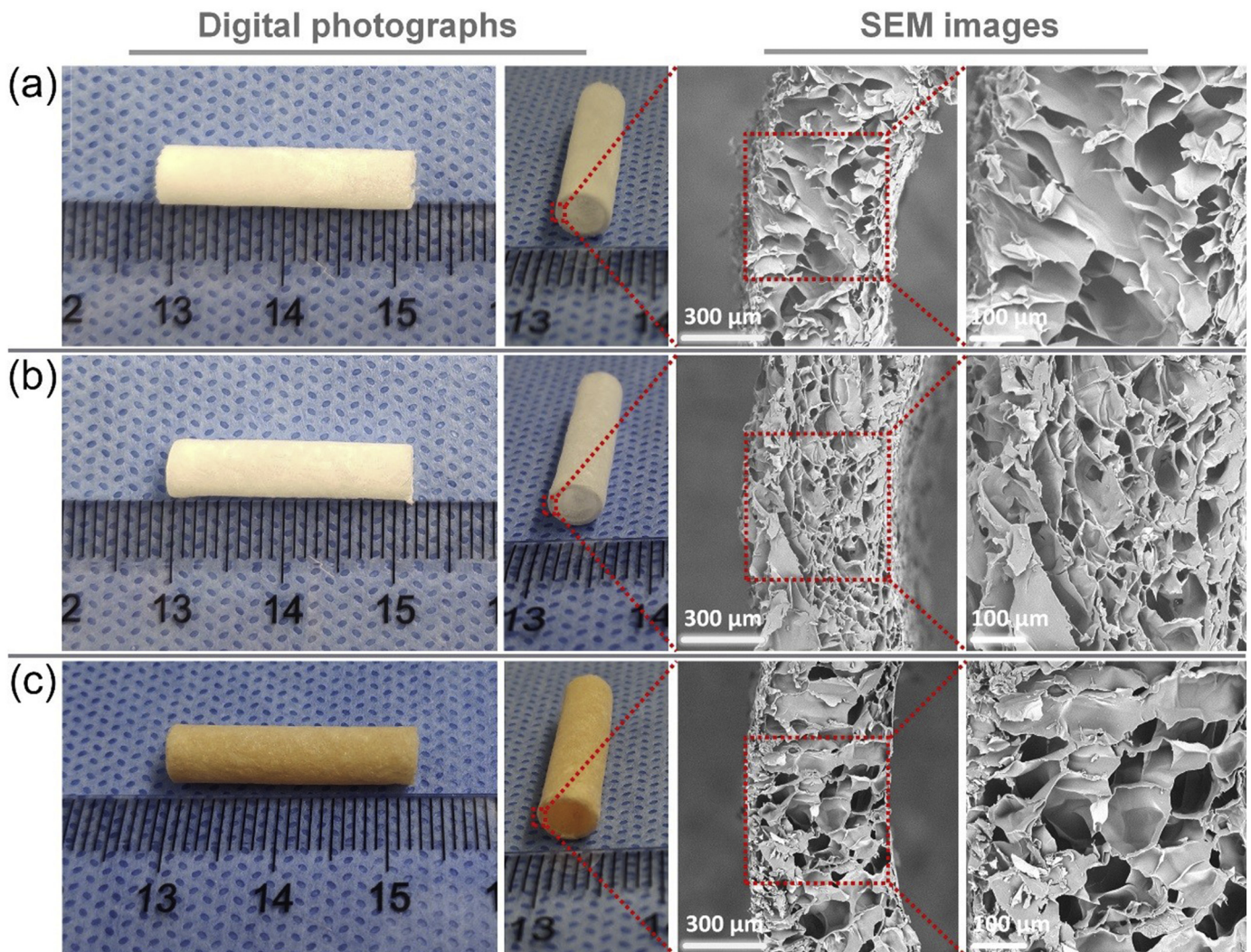


Fig. 2. Digital photographs and cross-sectional SEM images of scaffolds: (a) Gel-E/N tubular scaffold; (b) Gel-E/N-Hep tubular scaffold; (c) Gel@CS-Hep tubular scaffold.

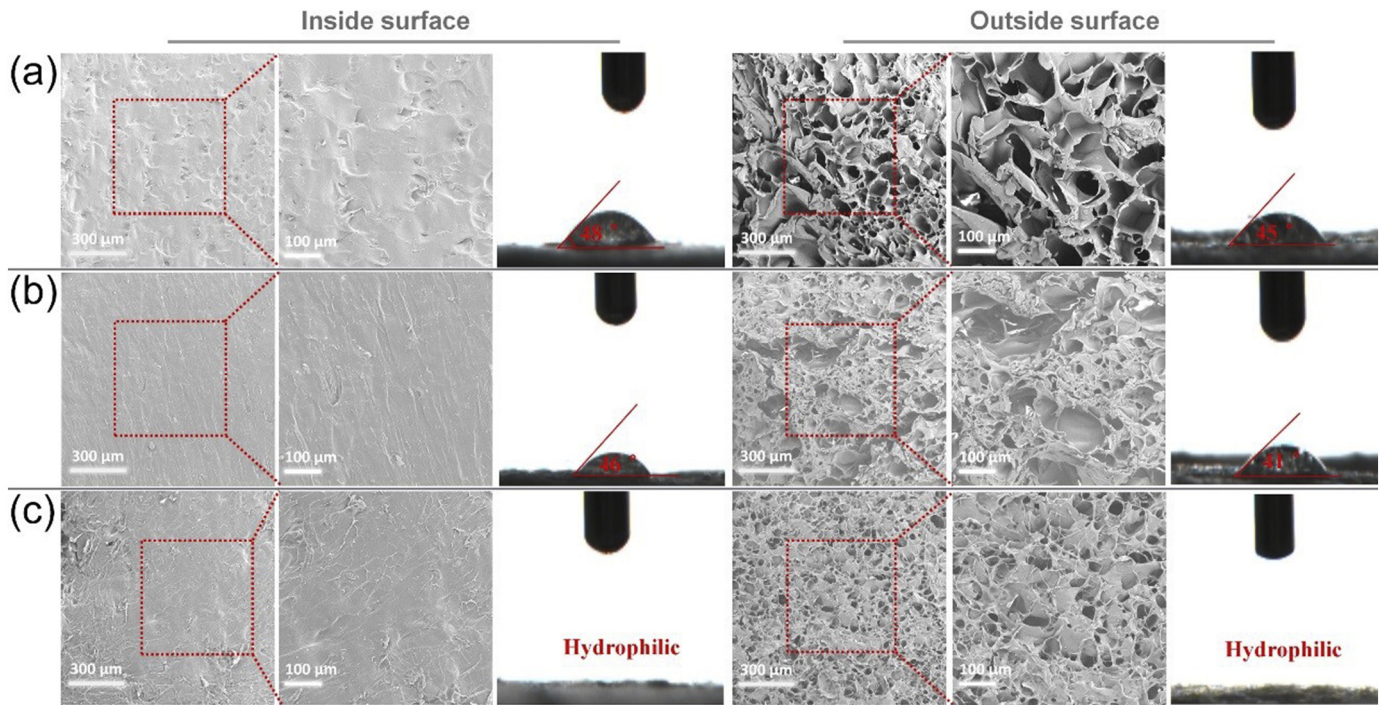


Fig. 3. SEM images of inside and outside surface and water contact angle (images of drops captured at 0.5 s) of scaffolds: (a) Gel-E/N tubular scaffold; (b) Gel-E/N-Hep tubular scaffold; (c) Gel@CS-Hep tubular scaffold.

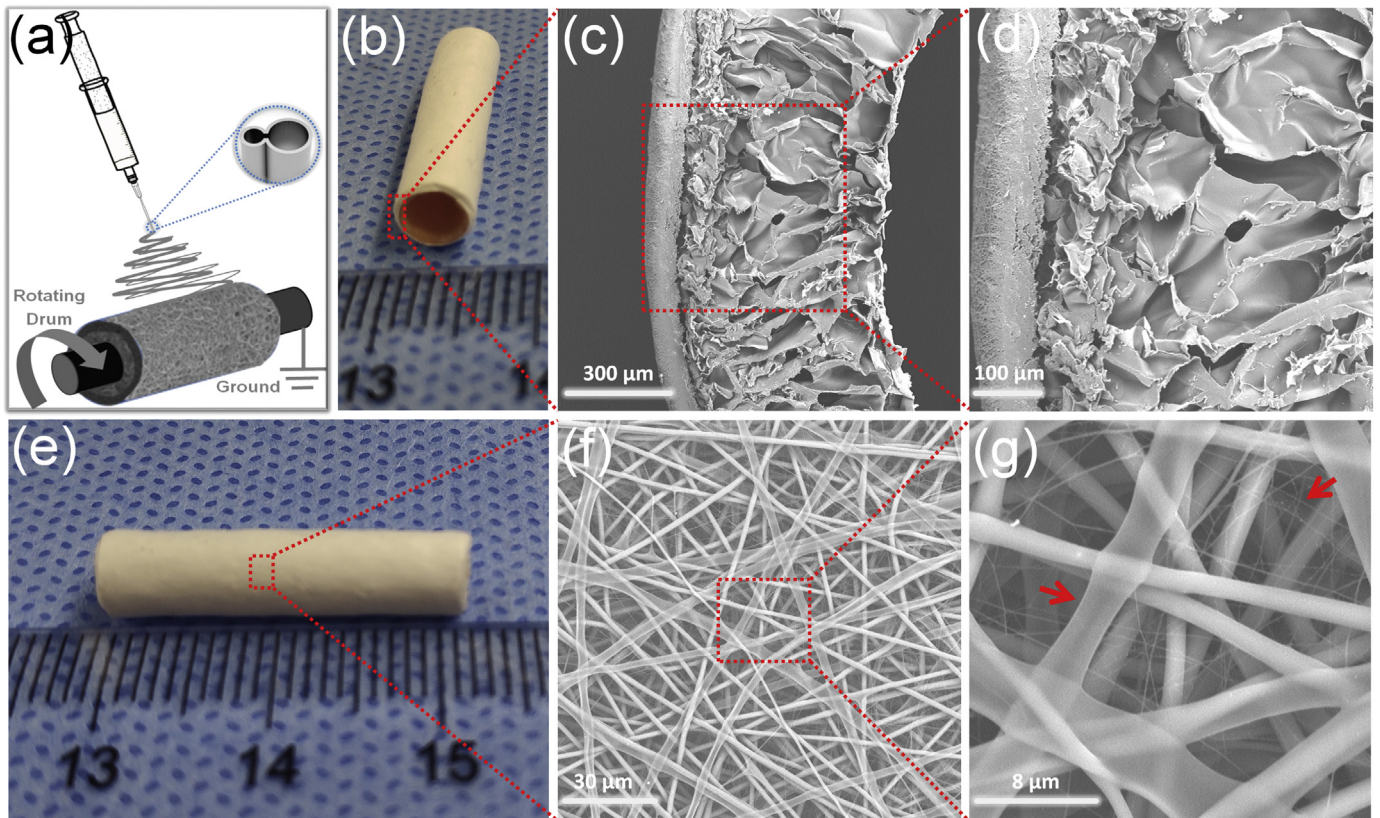


Fig. 4. (a) Schematic illustration of the fabrication of micro-nano fibers of the tubular scaffold using an “8”-type syringe needle; (b) Cross-sectional digital photographs, (c) and (d) cross-sectional SEM images, (e) digital photographs of outside surface, (f) and (g) surface SEM images of tubular scaffolds. The red arrows stand for microfiber and nanofiber, respectively.

scaffolds easily been damaged after grafting or crosslinking [34,35]. From Fig. 2, it can be seen that gelatin could easily be fabricated into tubular scaffolds with a three-dimensional microporous structure. The colour of Gel@CS-Hep tubular scaffold (Fig. 2c) appeared faint yellow, which mainly the colour of the chitosan coating on the gelatin, compared with Gel-E/N tubular scaffold (Fig. 2a) and Gel-E/N-Hep tubular scaffold (Fig. 2b). Compared the cross-sectional SEM images, Gel-E/N tubular scaffold, Gel-E/N-Hep tubular scaffold, and Gel@CS-Hep tubular scaffold displayed a porous structure with a pore size of about 50–80 μm , allowing for cell in-growth. All in all, there were no gross defects in the prepared Gel@CS-Hep tubular scaffold and it was macroscopically smooth, and the structures of the tube remain intact after the crosslinking and grafting process. The crosslinking and grafting process did not cause any visible morphological changes.

The microstructure of the inside and outside surface and surface wettability of Gel-E/N tubular scaffold, Gel-E/N-Hep tubular scaffold, and Gel@CS-Hep tubular scaffold were observed by SEM images and water contact angle, respectively, as shown in Fig. 3. It is obviously seen that three tubular scaffolds presented a smooth compact inner surface and a porous fluffy outer surface. The smooth compact inner surface would prevent blood oozing as well as the porous fluffy outer surface would conducive to the regeneration and growth of vascular smooth muscle cells. In Fig. 3c, the inside and outside surface for Gel@CS-Hep

tubular scaffold were presented super hydrophilic properties compared with the inside and outside surface of Gel-E/N tubular scaffold (Fig. 3a) and Gel-E/N-Hep tubular scaffold (Fig. 3b), suggesting that coating of chitosan might promote cell adhesion and migration.

Gel@CS-Hep/PU75 vascular scaffold was fabricated by electrospun PU75 micro-nanofibers out of the Gel@CS-Hep tube using an “8”-type syringe needle as shown in Fig. 4a. The morphology and dimensions of the Gel@CS-Hep/PU75 vascular scaffold were characterized by SEM (Fig. 4b-g). The two layers were tightly attached to each other without apparent delamination (Fig. 4c, d). The inner wall thickness was approximately 500 μm , and the wall thickness of the PU75 nanofibers was approximately 100 μm (Fig. 4b-d). Furthermore, the external PU75 layer showed a homogeneous fibrous morphology with two different diameter distributions of several tens and thousands of nanometers. The PU75 fibers provided sufficient and optimal mechanical properties, which can satisfy the requirement for artificial vascular replacement.

3.2. Chemical characterizations of crosslinking and grafting

Most researches were focused on the functionalization of intima of vascular scaffolds that remain in blending or on the electrostatic interaction between the carboxyl and primary amino groups [11,36–38].

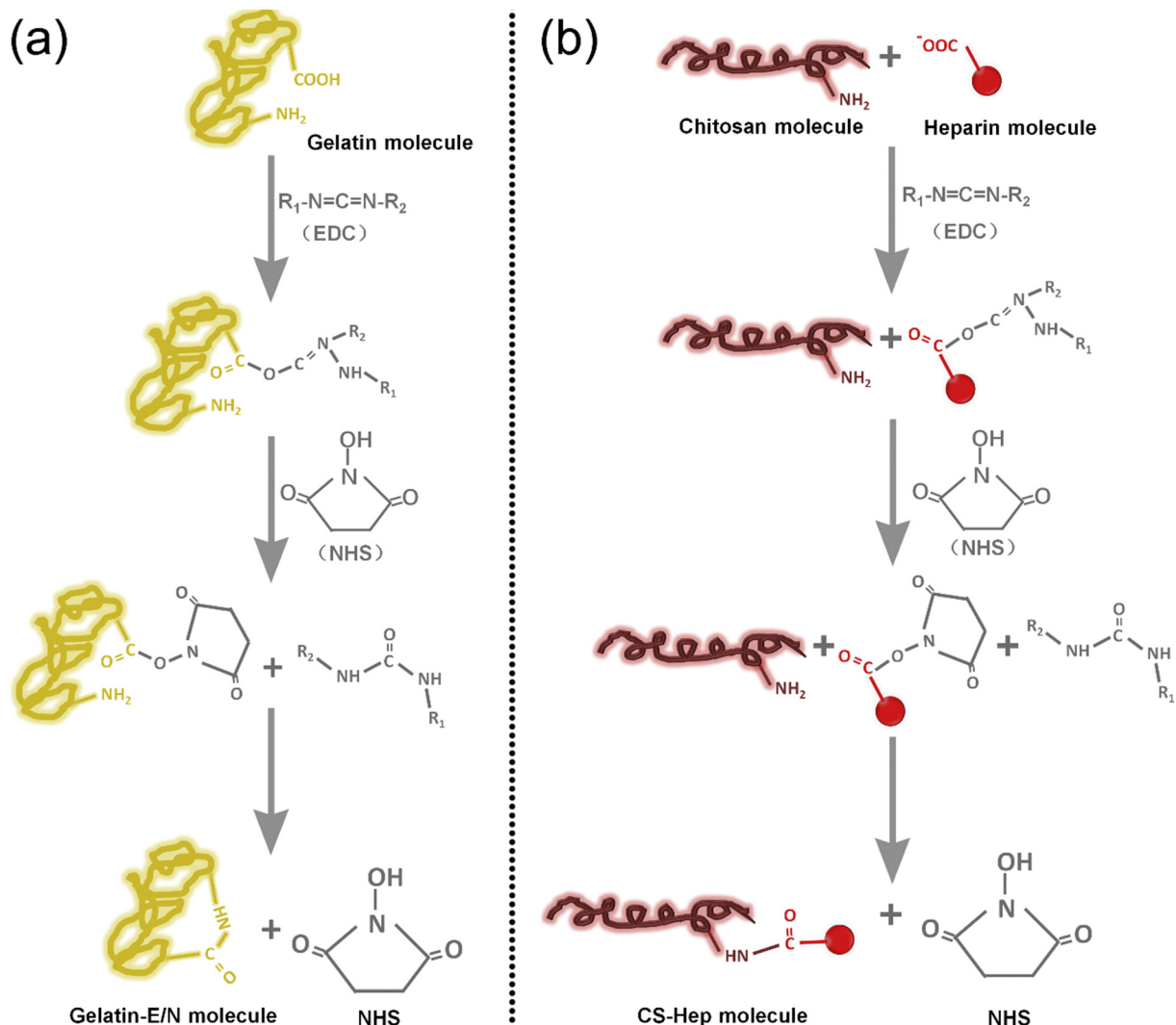


Fig. 5. Formation mechanisms of (a): Gelatin-E/N molecule crosslinking with EDC/NHS solution and (b) CS-Hep molecule: crosslinking and grafting with EDC/NHS/heparin solution.

However, most vascular scaffolds, which were intimal functionalization via the above methods, cannot be harvested effective results for transplantation. In the present research, unlike any other research and technology, two-step solution crosslinking modification was adopted to regulate the preparation of the three-dimensional porous tubular scaffolds with the formation mechanisms shown in Fig. 5. By separately controlling the molar ratio of the carboxyl and amino groups of gelatin, chitosan, and heparin, a stable three-dimensional tubular scaffold can be successfully prepared.

FTIR spectroscopy determines chemical bonds through the radiation of electromagnetic waves to recognize materials and their interactions in Fig. 6a–c. The characteristic peaks of the gelatin are observed at 1650 cm^{-1} and 1538 cm^{-1} for amide I and II, respectively. The spectrum confirmed the presence of C–O stretching at 1079 cm^{-1} of PEUU. The characteristic peaks at 3450 cm^{-1} or 1385 cm^{-1} were assigned to the amino of gelatin (Fig. 6a and Fig. 6c). The characteristic peaks at $2960\text{--}2860\text{ cm}^{-1}$ may to CH, CH₂ and CH₃ stretching of Gel, Gel-E/N, Gel-E/N-Hep, or Gel@CS-Hep, respectively, in Fig. 6b. The crystalline structural analysis of Gel, Gel-E/N, Gel-E/N-Hep, and Gel@CS-Hep composite was explored through as shown in Fig. 6d, where crystalline zones display diffuse diffraction peaks and amorphous regions show broader ones. For Gel@CS-Hep, the formation of amide bonds of gelatin, chitosan and heparin molecular chains during the crosslinking process also affect the crystallization. After crosslinking and grafting, the different peaks of Gel@CS-Hep at $2\theta = 30^\circ$ becomes stronger, which probably due to chitosan belong to the crystal materials, and the intermolecular crystal structure was hardly been destroyed.

Due to the insensitivity of the FTIR and WAXRD technique or the fact that the vibration bands of heparin are overlapped with those of chitosan or gelatin, toluidine blue staining of tubular scaffolds were used determined whether heparin was grafted in the vascular scaffold. Toluidine blue adsorption assay showed the colour of Gel@CS-Hep tubular scaffold changed from white to purple after heparin covalent immobilization, confirmed the immobilization of heparin in the vascular scaffolds as shown in Fig. 6e. The grafting concentration of heparin of

Gel, Gel-E/N, Gel-E/N-Hep, and Gel@CS-Hep tubular scaffolds were also quantified by toluidine blue assay [39], respectively, in Fig. 6f. The density of heparin on Gel, Gel-E/N, Gel-E/N-Hep, and Gel@CS-Hep vascular scaffolds were $0.26 \pm 0.13\text{ }\mu\text{g}/\text{mm}^3$, $1.01 \pm 0.11\text{ }\mu\text{g}/\text{mm}^3$ and $1.72 \pm 0.19\text{ }\mu\text{g}/\text{mm}^3$, respectively. Obviously, a relatively low amount of heparin was observed on the Gel-E/N tubular scaffold with the physical absorption of heparin from Fig. 6f. In addition, compared with the density of heparin on the Gel-E/N-Hep tubular scaffold, the amount of heparin on Gel@CS-Hep tubular scaffold was more, may due to the more active amino sites of chitosan, which brought more chances for chemical graft reaction. These results confirmed that the addition of chitosan could increase the load of heparin of scaffolds and positively affect the endothelialization and anticoagulation of scaffolds in vivo.

3.3. Mechanical properties of tubular scaffolds

For vascular replacement, the extreme challenge is to withstand the pressure of arterial blood flow after implantation in situ. For this reason, more replacements were prepared using materials with better mechanical properties [40,41]. However, the materials with better mechanical properties limited the growth of host cells due to the lasting degradation cycle. Therefore, we choose macroporous natural material as the inner layer of the vascular scaffold, which is beneficial to the previous growth of the host cell and nanofiber as the outer layer plays a role in mechanical support. Mechanically matched scaffolds are fundamental for vascular tissue regeneration. Representative radial stress-strain curves and Young's modulus of Gel-E/N tubular scaffold, Gel-E/N-Hep tubular scaffold, and Gel@CS-Hep tubular scaffold are presented in Fig. 7a, b. The results showed that the modulus of the Gel@CS-Hep tubular scaffold ($3.59 \pm 1.25\text{ MPa}$) was similar to that of radial arteries ($2.68 \pm 1.81\text{ MPa}$) [17]. It is clearly that Young's modulus of Gel-E/N-Hep tubular scaffold, and Gel@CS-Hep tubular scaffold significant decreased while compare with Gel-E/N tubular scaffold. After crosslinking, the molecular chain is wound more tightly, which increases the elasticity of the scaffold and reduces Young's modulus. The decrease of

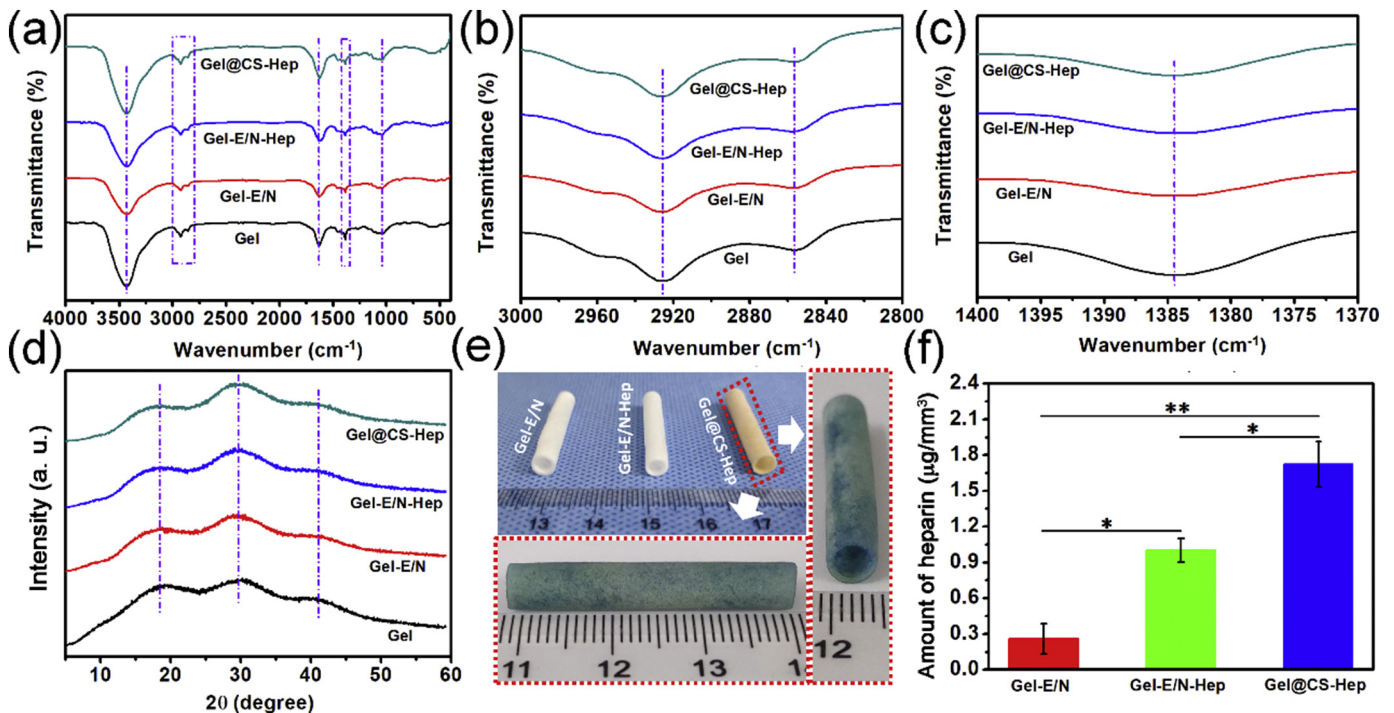


Fig. 6. (a)–(c) FTIR spectra curves and (d) X-ray diffraction pattern of Gel, Gel-E/N, Gel-E/N-Hep, and Gel@CS-Hep: (a) 400–4000 wavenumber range; (b) 2800–3000 wavenumber range; (c) 1370–1400 wavenumber range; (e) Digital photographs of Gel-E/N tubular scaffold, Gel-E/N-Hep tubular scaffold, and Gel@CS-Hep tubular scaffold (toluidine blue staining of Gel@CS-Hep tubular scaffold in wet states as indicated by the white arrow); (f) Density of heparin in the prepared tubular scaffolds.

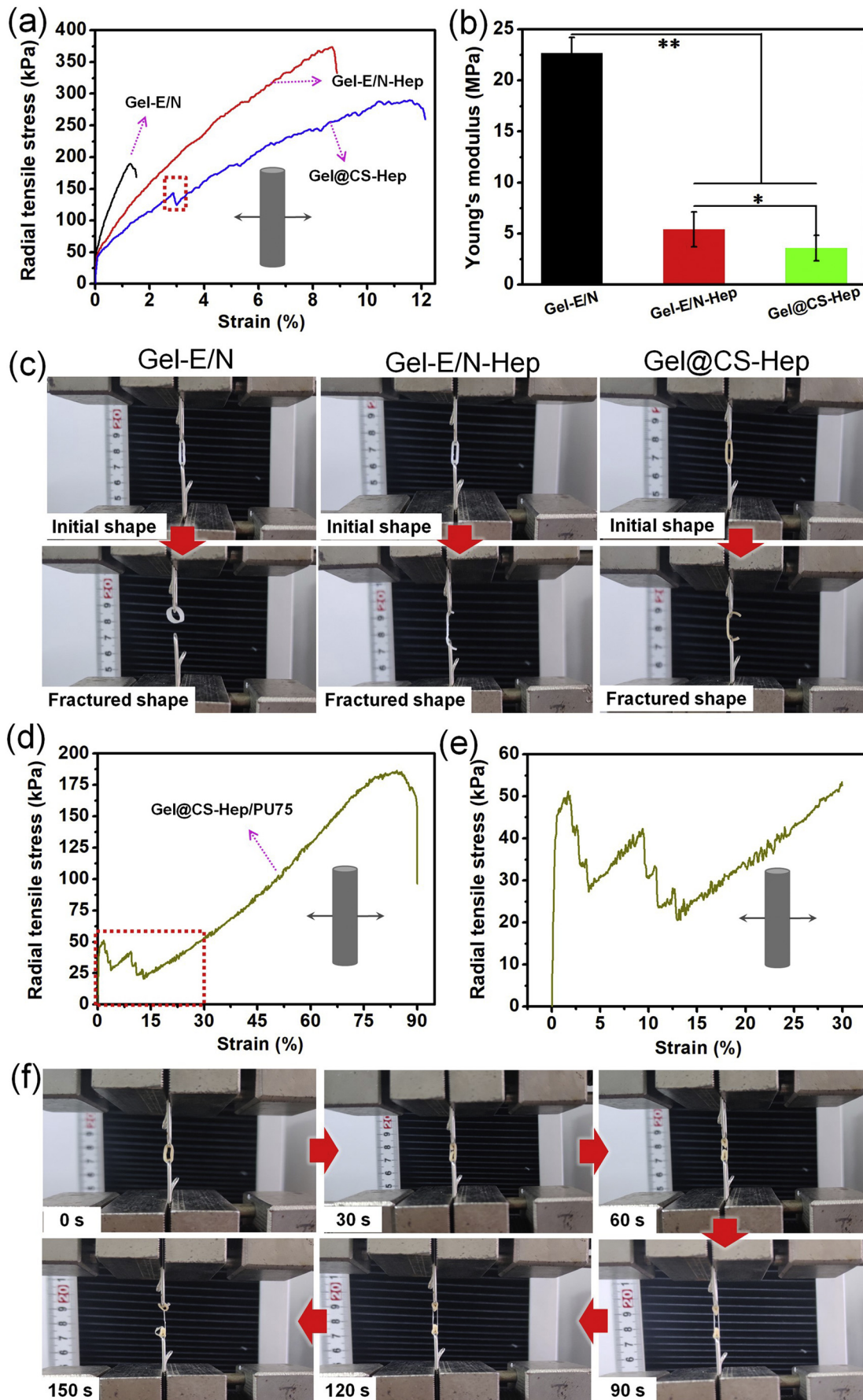


Fig. 7. Mechanical properties of prepared tubular scaffolds: representative radial tensile results of Gel-E/N tubular scaffold, Gel-E/N-Hep tubular scaffold, Gel@CS-Hep tubular scaffold, and Gel@CS-Hep/PU75 tubular scaffold under wet conditions: (a) radial stress-strain curves, (b) Young's modulus, (c) digital photographs of initial shape and fractured shape of Gel-E/N tubular scaffold, Gel-E/N-Hep tubular scaffold, and Gel@CS-Hep tubular scaffold; (d) and (e) radial stress-strain curves of Gel@CS-Hep/PU75 tubular scaffold, (f) digital photographs showing the shape change effect during radial stretching.

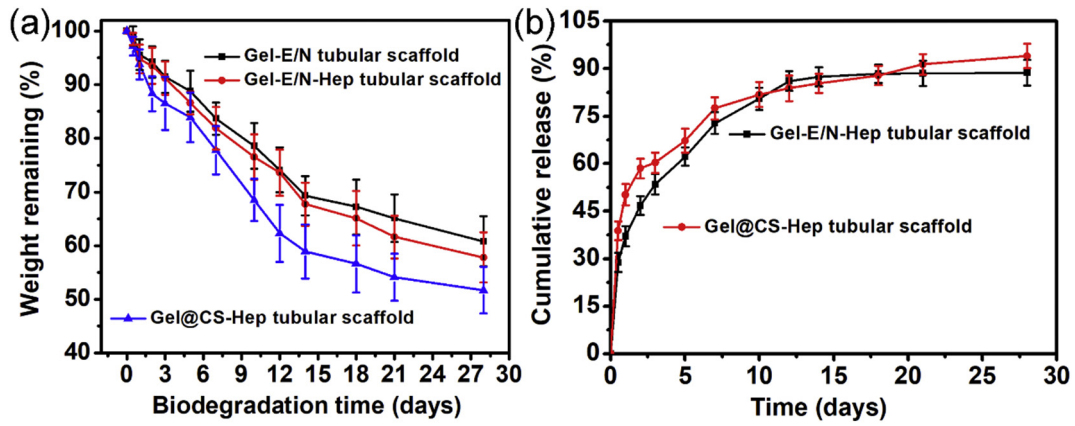


Fig. 8. (a) Mass remaining of Gel-E/N tubular scaffold, Gel-E/N-Hep tubular scaffold, and Gel@CS-Hep tubular scaffold immersed in pH = 7.4 PBS (n = 5); (b) In vitro releases of heparin from Gel-E/N-Hep tubular scaffold and Gel@CS-Hep tubular scaffold with similar mass of heparin in pH = 6.8 PBS (n = 5).

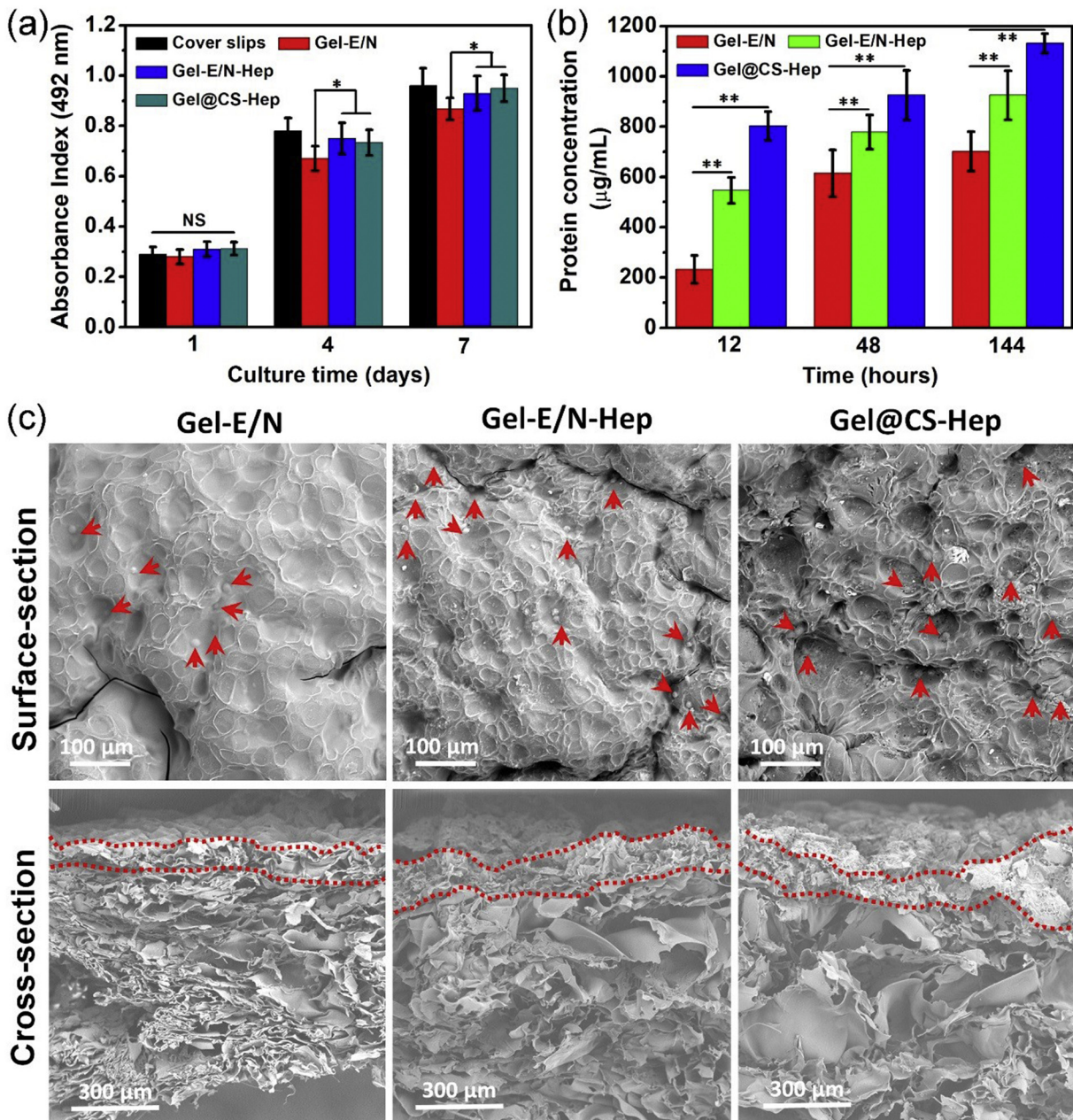


Fig. 9. (a) CCK-8 assay of the proliferation viability of HUVECs cultured onto coverslips, Gel-E/N tubular scaffold, Gel-E/N-Hep tubular scaffold, and Gel@CS-Hep tubular scaffold, respectively; (b) Protein adsorption results and (c) SEM images of Gel-E/N tubular scaffold, Gel-E/N-Hep tubular scaffold, and Gel@CS-Hep tubular scaffold after 4 days culture. Red arrows in (c) indicate the HUVECs.

Young's modulus also proves that scaffolds have good anti-deformation performance after implantation in vivo. As shown in Fig. 7c, the zone of breaks of scaffold is all located in the middle of the sample, which means this fracture test is effective. As the red frame is shown in Fig. 7a, the Gel@CS-Hep tubular scaffold showed two breaks, the first one occurred at 2.8% strain due to the break of the CS-Hep matrix, and the second break occurred around 11.8% strain, which stands for the break of gelatin matrix. Compared to Gel-E/N tubular scaffold, the crosslinking-grafting process leads to an prominent increase of tensile strength, Young's modulus and an obvious decrease of elongation at break of the Gel-E/N-Hep tubular scaffold and Gel@CS-Hep tubular scaffold in wet conditions. After crosslinking by EDC/NHS and heparin grafting, the tensile strength was about 290 kPa, which was less than Gel-E/N-Hep tubular scaffold. This may due to the dense molecular network structure that is formed during the crosslinking and grafting process, which changes the hardness of the tubular scaffold.

To further evaluate the mechanical properties of the Gel@CS-Hep/PU75 tubular scaffold, radial stretching was executed at a fixed rate of 0.05 mm/min (Fig. 7d, e). Gel@CS-Hep/PU75 tubular scaffold showed two fracture curves. The curve of the first stage presented a decreasing twisted trend and the curve of the second stage with a quick decreasing trend and finally rupture. Scilicet, the Gel@CS-Hep/PU75 bilayered tubular scaffold showed two obvious breaks, the first one occurred at 2.4%–13.0% strain due to the break of Gel@CS-Hep layer, and the second break occurred at around 83.0% strain, which stands for the break of PU75 nanofiber layer. In a word, the results of this part about the Gel@CS-Hep/PU75 tubular scaffold indicated that the mechanical properties are close to the biomechanics of natural vessels, which plays a key role in maintaining long-term patency after transplant.

3.4. Degradation in vitro and heparin sustained release properties

The degradation properties of the Gel-E/N tubular scaffold, Gel-E/N-Hep tubular scaffold, and Gel@CS-Hep tubular scaffold were tested after immersed in pH = 7.4 PBS. As shown in Fig. 8a, there was approximately 49% mass loss for Gel@CS-Hep tubular scaffold degraded in 28 days, while there was nearly 40% and 43% mass loss for Gel-E/N tubular scaffold and Gel-E/N-Hep tubular scaffold, respectively. The degradation process of the Gel@CS-Hep tubular scaffold contains three stages: the erosion of chitosan, skeleton fracture of the gelatin tubular scaffold and the overall collapse of the scaffold. A dramatic decrease in weight before day 2 could be due to the fracture of the molecular chain between chitosan, which coating on the surfaces of the gelation skeleton. The weight decreased rapidly from approximately the fifth day to the fourteenth day, which can be attributed to the decomposition of the main structure of the scaffold. For chemically grafted scaffolds, the degradation properties and drug release profiles are closely linked.

For the sustained release of heparin, PBS with a pH of 6.8 was adopted. This is because human blood tends to be acidic when thrombus and other vascular diseases occur, and the release rate of heparin under this condition is more representative. By simulating the heparin release effect in such extreme cases, we demonstrated that the designed scaffold was effective in pathological environment. As illustrated in Fig. 8b, more than 50% of loaded heparin was released on the third day. After that, the Gel@CS-Hep tubular scaffold demonstrated a faster release in comparison with Gel-E/N-Hep tubular scaffold in 7 days about 78% loaded heparin was released. Tracing back to the heparin-loading efficiency of the Gel@CS-Hep tubular scaffold in Fig. 6f, this tubular scaffold will be an effective artificial intima to resist acute coagulation.

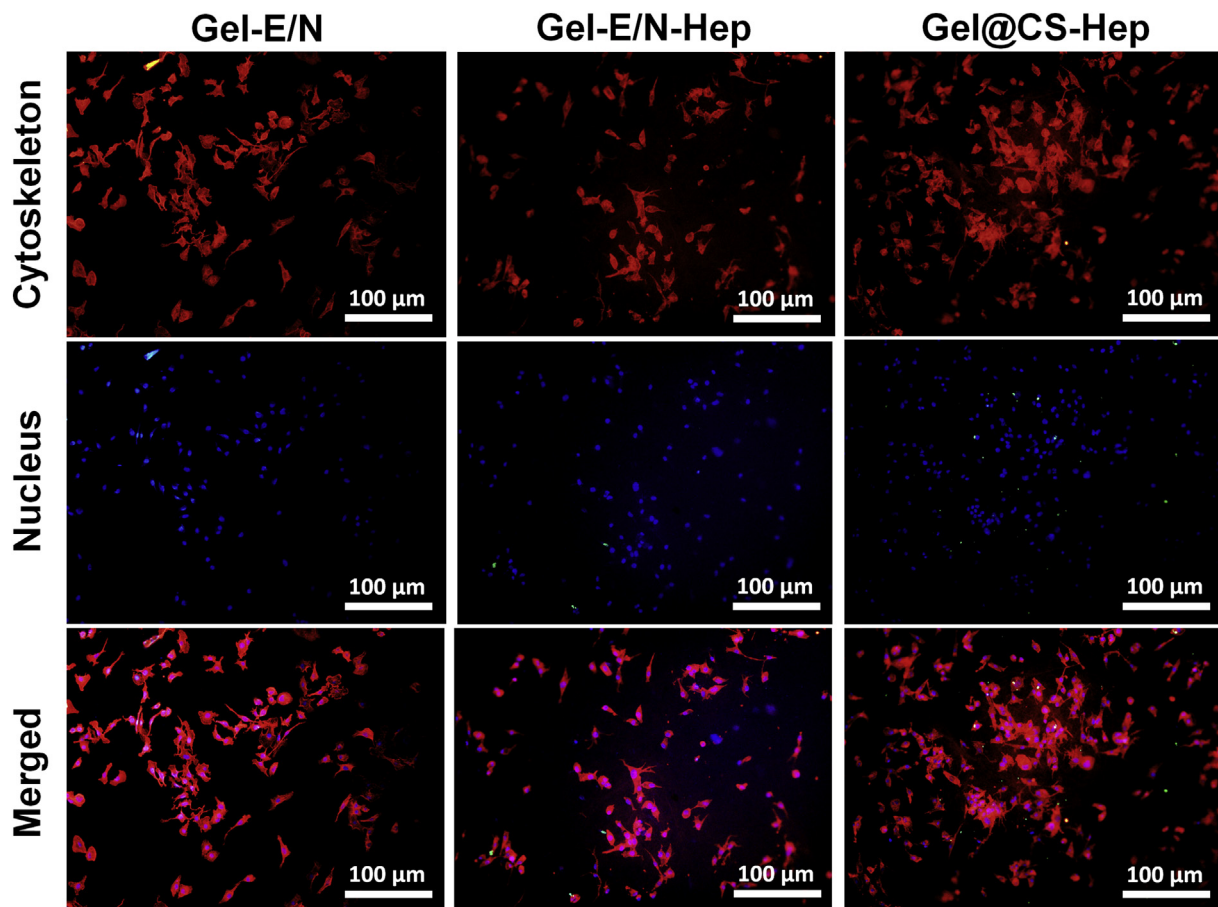


Fig. 10. DAPI (blue)/rhodamine-conjugated phalloidin (red) staining assay of HUVECs cells on the surfaces of Gel-E/N scaffold, Gel-E/N-Hep scaffold, and Gel@CS-Hep scaffold after culturing for 2 days, respectively.

3.5. Biocompatibility assay of the prepared tubular scaffolds in vitro

Although gelatin possessed good biocompatibility, the introduction of a crosslinking will increase the cytotoxicity of the prepared tubular scaffold during crosslinking [18]. Some studies have also confirmed that the residue of the crosslinking inside scaffolds would limit cell proliferation and migration. So it is necessary to test the biocompatibility of the developed Gel@CS-Hep tubular scaffold. In vitro proliferation measured by CCK-8 assay of human umbilical vein endothelial cells (HUVECs) after 1, 4, and 7 days after cultured on the surfaces of Gel-E/N tubular scaffold, Gel-E/N-Hep tubular scaffold, and Gel@CS-Hep tubular scaffold ($n = 3$ for each group) is shown in Fig. 9a. From the histogram, HUVECs adhered to the surfaces of all tubular scaffolds and coverslips without a significant difference in cell numbers after one day of culture. After four days or seven days of culture, the number of viable cells on both the Gel-E/N-Hep tubular scaffold and the Gel@CS-Hep tubular scaffold was more than that on the Gel-E/N tubular scaffold. Protein plays an important role in cell survival and adhesion, Fig. 9b shows the results of protein adsorption of all tubular scaffolds. The protein adsorption of all tubular scaffolds increased as time goes on. Compared with Gel-E/N tubular scaffold and Gel-E/N-Hep tubular scaffold, Gel@CS-Hep tubular scaffold was able to absorb more protein at the same

time, indicating that Gel@CS-Hep tubular scaffold possessed stronger sustained protein absorption ability. Link with the morphology and wettability results of tubular scaffolds in Fig. 2 and Fig. 3, which may be due to the fact that during the long-term contact with the protein, Gel@CS-Hep tubular scaffold is more likely to absorb the protein into the inside of scaffold, while the proteins are mostly located on the surface of other scaffolds.

Fig. 9c shows surface and cross-section SEM images of HUVECs proliferation after seeding on different scaffolds at days 4 culture. It can be seen that the HUVECs were equally deposited onto the surfaces of scaffolds (as red arrows indicated). From cross-section SEM images, a thin layer of cells has formed on the surface of tubular scaffolds as well as the wall of tubular scaffolds still maintains the three-dimensional porous structure.

In Fig. 10, from the fluorescence microscopy staining images for day 2 of HUVECs proliferation, the cells have a similar shape, and the cells on the surfaces of the Gel@CS-Hep tubular scaffold are spread more homogeneously, as well as presenting more pseudopods. After 4 days culture, the number of cells of the Gel@CS-Hep tubular scaffold was statistically significant ($*p < .05$) compared with Gel-E/N tubular scaffold and Gel-E/N-Hep tubular scaffold, indicating that Gel@CS-Hep tubular scaffold enhanced cell growth and proliferation. This may be due to the existence of

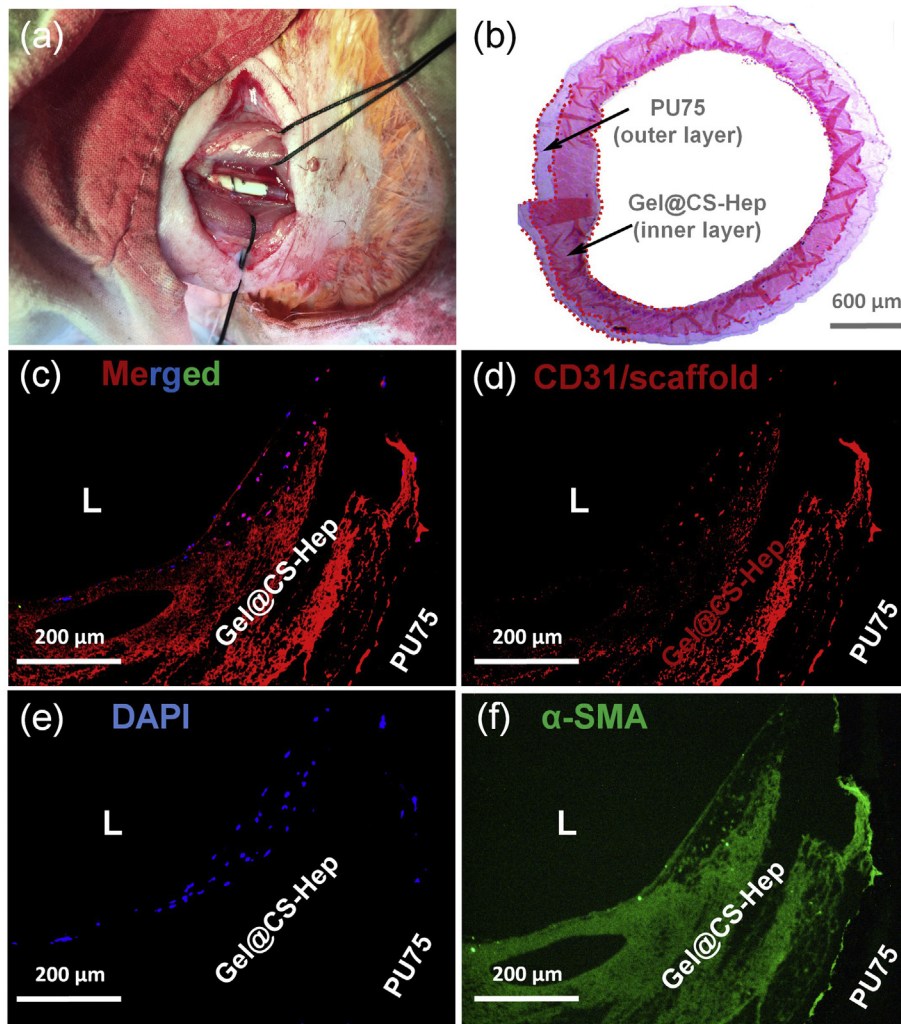


Fig. 11. (a) Surgical implantation of Gel@CS-Hep/PU75 bilayered tubular scaffold implanted in rabbit carotid artery; (b) H&E staining image, (c)-(f) immunofluorescent staining images of Gel@CS-Hep/PU75 bilayered tubular scaffold for 14 days implantation (red = CD31/scaffold; blue = nucleus; green = α -SMA). Black arrows in (b) indicate the outer layer and inner layer and red dashed shiny lines indicate the boundary of outer layer and inner layer of implanted tube; "L" indicates lumen in (c)-(f).

amino on the surfaces of chitosan which provides a positive charge site for facilitating cell attachment as well as the three-dimensional porous structure of the Gel@CS-Hep tubular scaffold is similar to the skeleton of the extracellular matrix, which is adapt for cell growth. This is also evident from SEM micrographs of the Gel@CS-Hep tubular scaffold exhibiting uniform porosity in Fig. 2 and Fig. 3, which is the prerequisite for the proliferation of cells over the scaffold material.

3.6. Anti-coagulation and endothelialization after transplantation in situ

The prepared Gel@CS-Hep/PU75 bilayered tubular scaffold with good suitability and pliability under wet conditions has been replaced onto the rabbit's carotid artery for effective end-to-end anastomosis. Fig. 11a exhibits the surgical implantation of the Gel@CS-Hep/PU75 bilayered tubular scaffold with a size of 2 mm in inner diameter and 10 mm in length into the carotid artery of a New Zealand white rabbit. The two-dimensional Doppler performed to evaluate the patency rate showed that all 10 (100%) Gel@CS-Hep/PU75 bilayered tubular scaffold (Fig. S1) was patent. Hematoxylin and eosin (H&E) staining image implanted for 14 days presented in Fig. 11b. At 14 days, the intercommunicating macroporous structure of the scaffold allowed extensive blood penetration into the inner layer of the scaffold wall (as shown in the middle of the red dotted line), which will provide a favorable microenvironment for endothelial cells adhesion. In order to detect the formed vascular tissue, immunofluorescent staining for endothelial cells and smooth muscle cells were performed. Immunostaining confirmed that the lumen of the scaffold was completely covered by CD31 positive cells (Fig. 11c-e), which was similar to the native arteries' arrangement [42], although its compactness was lower than that in native arteries (Fig. S2). These experimental results indicate that such a bilayered tubular scaffold shows the potential favorable rapid endothelialization performance for anti-acute thrombosis, though the smooth muscle layer cannot be reconstructed quickly (Fig. 11f).

4. Conclusion

In summary, in the present work, a new functional Gel@CS-Hep/PU75 bilayered tubular scaffold composed of fluffy interlayer was prepared. The inter layered of functional tubular scaffold shows 0° water contact angle at 0.5 s, mechanical properties close to native vessels' with a similar radial stress-strain curves and Young's modulus of 3.59 ± 1.25 MPa, as well as a porous structure with a pore size of about 50–80 μm conducive to cell growth. More importantly, the heparinized microstructure could induce rapid adhesion of endothelial cells in vivo, in which the regenerated tunica intima was well organized on the surfaces of the scaffolds the lumen of the scaffold that is similar to the native arteries. This new strategy may bring cell-free small-diameter vascular scaffolds closer to clinical application, providing a new possibility for clinical small vessel transplantation.

Supplementary data to this article can be found online at <https://doi.org/10.1016/j.matdes.2020.108943>.

Author contributions

WC Yao, tubular scaffold design. HB Gu, culture cells. T Hong and Y Wang, animal operation. WY Li, SEM test. SH Chen, mechanical test. CS Wang and XM Mo, review. SY Lu and TH Zhu, funding acquisition and review & editing.

Notes

The authors declare no competing financial interest.

Declaration of Competing Interest

None.

Acknowledgements

The authors sincerely appreciate projects funded by “National Natural Science Foundation of China (Grant No.81501595, 81902186, 81671920, 31972923, 81871753, 81772341)”, “National Key Research and Development Program of China (Grant No. 2018YFC1106200, 2018YFC1106201, 2018YFC1106202)”, “Technology Support Project of Science and Technology Commission of Shanghai Municipality of China (Grant No. 19441901700, 19441901701, 19441901702, 18441902800)”, Shanghai Rising-Star Program (20QC1401300)”, Shanghai Post-doctoral Excellence Program (2019365) and “China Post-doctoral Science Foundation (Grant No. 2019M661525)”. We extend appreciation to Dr. Jinglei Wu, Binbin Sun, and Dr. Juan Du for technical support and expertise.

Credit Author Statement

All authors have made substantial contributions to the present work. WC Yao, tubular scaffold design. HB Gu, culture cells. T Hong and Y Wang, animal operation. WY Li, SEM test. SH Chen, mechanical test. CS Wang and XM Mo, review. SY Lu and TH Zhu, funding acquisition and review & editing.

References

- [1] Q.L. Zhao, J. Wang, H.Q. Cui, H.X. Chen, Y.L. Wang, X.M. Du, Programmed shape-morphing scaffolds enabling facile 3D endothelialization, *Adv. Funct. Mater.* 28 (29) (2018) 1801027.
- [2] J.Y. Yang, K.Y. Wei, Y.Q. Wang, Y.Z. Li, N. Ding, D. Huo, T.R. Wang, G.Y. Yang, M.C. Yang, T. Ju, W. Zeng, C.H. Zhu, Construction of a small-caliber tissue-engineered blood vessel using icariin-loaded-cyclodextrin sulfate for in situ anticoagulation and endothelialization, *Sci. China-Life Sci.* 61 (10) (2018) 1178–1188.
- [3] J. Zhao, L.C. Bai, X.-K. Ren, J.T. Guo, S.H. Xia, W.C. Zhang, Y.K. Feng, Co-immobilization of ACH11 antithrombotic peptide and CAG cell-adhesive peptide onto vascular grafts for improved hemocompatibility and endothelialization, *Acta Biomater.* 97 (2019) 344–359.
- [4] L.Z. Kang, W.B. Jia, M. Li, Q. Wang, C.D. Wang, Y. Liu, X.P. Wang, L. Jin, J.J. Jiang, G.F. Gu, Z.G. Chen, Hyaluronic acid oligosaccharide-modified collagen nanofibers as vascular tissue-engineered scaffold for promoting endothelial cell proliferation, *Carbohydr. Polym.* 223 (2019) 115106.
- [5] M. Hamidi, M. Zeeshan, N. Kulvatunyou, H.S. Mitra, K. Hanna, A. Tang, A. Northcutt, T. O'Keefe, B. Joseph, Operative spinal trauma: Thromboprophylaxis with low molecular weight heparin or a direct oral anticoagulant, *J. Thromb. Haemost.* 17 (6) (2019) 925–933.
- [6] M.K. Phelps, T.E. Wiczer, H.P. Erdeljac, K.R. Van Deusen, K. Porter, G. Philips, T.F. Wang, A single center retrospective cohort study comparing low-molecular-weight heparins to direct oral anticoagulants for the treatment of venous thromboembolism in patients with cancer—a real world experience, *J. Oncol. Pharm. Pract.* 25 (4) (2019) 261–268.
- [7] E.M. Uppuluri, K.R. Burke, C.M. Haaf, N.L. Shapiro, Assessment of venous thromboembolism treatment in patients with cancer on low molecular weight heparin, warfarin, and the direct oral anticoagulants, *J. Oncol. Pharm. Pract.* 25 (2) (2019) 261–268.
- [8] T. Wang, X.Y. Ji, L. Jin, Z.Q. Feng, J.H. Wu, J. Zheng, Y. Wang, Z.W. Xu, L.L. Guo, N.Y. He, Fabrication and characterization of heparin-grafted poly-L-lactic acid-chitosan core-shell nanofibers scaffold for vascular gasket, *ACS Appl. Mater. Interfaces* 5 (9) (2013) 3757–3763.
- [9] Z.Q. Xu, Y.Q. Gu, J.X. Li, Z.G. Feng, L.R. Guo, Z. Tong, L. Ye, C.M. Wang, R. Wang, X. Geng, C. Wang, J. Zhang, Vascular remodeling process of heparin-conjugated poly(epsilon-caprolactone) scaffold in a rat abdominal aorta replacement model, *J. Vasc. Res.* 55 (6) (2018) 338–349.
- [10] W.Z. Wang, D.H. Liu, D.J. Li, H.B. Du, J.T. Zhang, Z.W. You, M.Q. Li, C.L. He, Nanofibrous vascular scaffold prepared from miscible polymer blend with heparin/stromal cell-derived factor-1 alpha for enhancing anticoagulation and endothelialization, *Colloids Surf. B* 181 (2019) 963–972.
- [11] J. Cao, X. Geng, J. Wen, Q.X. Li, L. Ye, A.Y. Zhang, Z.G. Feng, L.R. Guo, Y.Q. Gu, The penetration and phenotype modulation of smooth muscle cells on surface heparin modified poly(epsilon-caprolactone) vascular scaffold, *J. Biomed. Mater. Res. A* 105 (10) (2017) 2806–2815.
- [12] W. Wu, R.A. Allen, Y.D. Wang, Fast-degrading elastomer enables rapid remodeling of a cell-free synthetic graft into a neoartery, *Nat. Med.* 18 (7) (2012) 1148–1153.
- [13] X. Yang, J.H. Wei, D.L. Lei, Y.P. Liu, W. Wu, Appropriate density of PCL nano-fiber sheath promoted muscular remodeling of PGS/PCL grafts in arterial circulation, *Biomaterials* 88 (2016) 34–47.
- [14] E. Anitua, P. Nurden, R. Prado, A.T. Nurden, S. Padilla, Autologous fibrin scaffolds: when platelet- and plasma-derived biomolecules meet fibrin, *Biomaterials* 192 (2019) 440–460.

- [15] P. Losi, L. Mancuso, T. Al Kayal, S. Celi, E. Briganti, A. Gualerzi, S. Volpi, G. Cao, G. Soldani, Development of a gelatin-based polyurethane vascular graft by spray, phase-inversion technology, *Biomed. Mater.* 10 (4) (2015), 045014.
- [16] N. Nagiah, R. Johnson, R. Anderson, W. Elliott, W. Tan, Highly compliant vascular grafts with gelatin-sheathed coaxially structured nanofibers, *Langmuir* 31 (47) (2015) 12993–13002.
- [17] S.K. Norouzi, A. Shamloo, Bilayered heparinized vascular graft fabricated by combining electrospinning and freeze drying methods, *Mater. Sci. Eng. C-Mater.* 94 (2019) 1067–1076.
- [18] H.Y. Wang, Y.K. Feng, H.Y. Zhao, R.F. Xiao, J. Lu, L. Zhang, J.T. Guo, Electrospun hemocompatible PU/gelatin-heparin nanofibrous bilayer scaffolds as potential artificial blood vessels, *Macromol. Res.* 20 (4) (2012) 347–350.
- [19] H.Y. Ma, J. Hu, P.X. Ma, Polymer scaffolds for small-diameter vascular tissue engineering, *Adv. Funct. Mater.* 20 (17) (2010) 2833–2841.
- [20] N. Kasoju, D. Kubies, M.M. Kumorek, J. Kříž, E. Fábryová, L. Machová, J. Kovářová, F. Rypáček, Dip TIPS as a facile and versatile method for fabrication of polymer foams with controlled shape, size and pore architecture for bioengineering applications, *PLoS One* 9 (9) (2014), e108792.
- [21] K. Yu, X.X. Zhou, T.H. Zhu, T. Wu, J. Wang, J. Fang, M.R. El-Aassar, H. El-Hamshary, M. El-Newehy, X.M. Mo, Fabrication of poly(ester-urethane) urea elastomer/gelatin electrospun nanofibrous membranes for the potential application in skin tissue engineering, *RSC Adv.* 6 (2016) 73636–73644.
- [22] D.L. Chen, J.J. Cao, J. Wang, M.F. Maitz, L. Guo, Y.C. Zhao, Q.L. Li, K.Q. Xiong, N. Huang, Biofunctionalization of titanium with PEG and anti-CD34 for hemocompatibility and stimulated endothelialization, *J. Colloid Interface Sci.* 368 (1) (2012) 636–647.
- [23] L. Ying, C. Yin, R.X. Zhuo, K.W. Leong, H.Q. Mao, E.T. Kang, K.G. Neoh, Immobilization of galactose ligands on acrylic acid graft-copolymerized poly(ethylene terephthalate) film and its application to hepatocyte culture, *Biomacromolecules* 4 (1) (2003) 157–165.
- [24] H.B. Du, L. Tao, W.Z. Wang, D.H. Liu, Q.Q. Zhang, P. Sun, S.G. Yang, C.L. He, Enhanced biocompatibility of poly(L-lactide-co-epsilon-caprolactone) electrospun vascular grafts via self-assembly modification, *Mater. Sci. Eng. C-Mater.* 100 (2019) 845–854.
- [25] W.Z. Wang, W. Nie, D.H. Liu, H.B. Du, X.J. Zhou, L. Chen, H.S. Wang, X.M. Mo, L. Li, C.L. He, Macroporous nanofibrous vascular scaffold with improved biodegradability and smooth muscle cells infiltration prepared by dual phase separation technique, *Int. J. Nanomedicine* 13 (2018) 7003–7018.
- [26] X.R. Guo, J.J. Zhu, H.M. Zhang, Z.W. You, Y. Morsi, X.M. Mo, T.H. Zhu, Facile preparation of a controlled-release tubular scaffold for blood vessel implantation, *J. Colloid Interface Sci.* 539 (2019) 351–360.
- [27] T.H. Zhu, K. Yu, M.A. Bhutto, X.R. Guo, J. Wang, W.M. Chen, H. El-Hamshary, S.S. Al-Deyab, X.M. Mo, Synthesis of RGD-peptide modified poly(ester-urethane) urea electrospun nanofibers as a potential application for vascular tissue engineering, *Chem. Eng. J.* 315 (2017) 177–190.
- [28] J.S. Choi, Y.X. Piao, T.S. Seo, Circumferential alignment of vascular smooth muscle cells in a circular microfluidic channel, *Biomaterials* 35 (1) (2014) 63–70.
- [29] D. Liu, T. Xiang, T. Gong, T. Tian, X. Liu, S.B. Zhou, Bioinspired 3D multilayered shape memory scaffold with a hierarchically changeable micropatterned surface for efficient vascularization, *ACS Appl. Mater. Interfaces* 9 (23) (2017) 19725–19735.
- [30] T. Vieira, J.C. Silva, J.P. Borges, C. Henriques, Synthesis, electrospinning and in vitro test of a new biodegradable gelatin-based poly(ester urethane urea) for soft tissue engineering, *Eur. Polym. J.* 103 (2018) 271–281.
- [31] R. van Lith, E.K. Gregory, J. Yang, M.R. Kibbe, G.A. Ameer, Engineering biodegradable polyester elastomers with antioxidant properties to attenuate oxidative stress in tissues, *Biomaterials* 35 (28) (2014) 8113–8122.
- [32] J.X. Wu, C.M. Hu, Z.C. Tang, Q. Yu, X.L. Liu, H. Chen, Tissue-engineered vascular grafts: balance of the four major requirements, *Colloid Inter. Sci. Commun.* 23 (2018) 34–44.
- [33] E.K. Gregory, A. Webb, J.M. Vercammen, M.E. Kelly, B. Akar, R. van Lith, E.M. Bahnsen, W.L. Jiang, G.A. Ameer, M.R. Kibbe, Inhibiting intimal hyperplasia in prosthetic vascular grafts via immobilized all-trans retinoic acid, *J. Control. Release* 274 (2018) 69–80.
- [34] D.G. Petlin, S.I. Tverdokhlebov, Y.G. Anissimov, Plasma treatment as an efficient tool for controlled drug release from polymeric materials: a review, *J. Control. Release* 266 (2017) 57–74.
- [35] E.N. Bolbasov, P.V. Maryin, K.S. Stankevich, A.I. Kozelskaya, E.V. Shesterikov, Yu.I. Khodyrevskaya, M.V. Nasonova, D.K. Shishkova, Yu.A. Kudryavtseva, Y.G. Anissimov, S.I. Tverdokhlebov, Surface modification of electrospun poly-(l-lactic) acid scaffolds by reactive magnetron sputtering, *Colloids Surf. B: Biointerfaces* 162 (2018) 43–51.
- [36] W.S. Choi, Y.K. Joung, Y. Lee, J.W. Bae, H.K. Park, Y.H. Park, J.-C. Park, K.D. Park, Enhanced patency and endothelialization of small-caliber vascular grafts fabricated by coimmobilization of heparin and cell-adhesive peptides, *ACS Appl. Mater. Interfaces* 8 (7) (2016) 4336–4346.
- [37] X.F. Qiu, B.L.-P. Lee, X.H. Ning, N. Murthy, N.G. Dong, S. Li, End-point immobilization of heparin on plasma-treated surface of electrospun polycarbonate-urethane vascular graft, *Acta Biomater.* 51 (2017) 138–147.
- [38] T.H. Zhu, J. Jiang, J.Z. Zhao, S.H. Chen, X.Y. Yan, Regulating preparation of functional alginate-chitosan three-dimensional scaffold for skin tissue engineering, *Int. J. Nanomedicine* 14 (2019) 8891–8903.
- [39] J. Lee, J.J. Yoo, A. Atala, S.J. Lee, Controlled heparin conjugation on electrospun poly(epsilon-caprolactone)/gelatin fibers for morphology-dependent protein delivery and enhanced cellular affinity, *Acta Biomater.* 8 (7) (2012) 2549–2558.
- [40] K. Liu, N. Wang, W.S. Wang, L.X. Shi, H. Li, F.Y. Guo, L.H. Zhang, L. Kong, S.T. Wang, Y. Zhao, A bio-inspired high strength three-layer nanofiber vascular graft with structure guided cell growth, *J. Mater. Chem. B* 5 (2017) 3758–3764.
- [41] C.W. Lou, P.C. Lu, J.J. Hu, J.H. Lin, Effects of yarn types and fabric types on the compliance and bursting strength of vascular grafts, *J. Mech. Behav. Biomed.* 59 (2016) 474–483.
- [42] M.F. Zhu, Z.H. Wang, J.M. Zhang, L.N. Wang, X.H. Yang, J.R. Cheng, G.W. Fan, S.L. Ji, C. Xing, K. Wang, Q. Zhao, Y. Zhu, D.L. Kong, L.Y. Wang, Circumferentially aligned fibers guided functional neoartery regeneration in vivo, *Biomaterials* 61 (2015) 85–94.